Observation of $\pi^- K^+$ and $\pi^+ K^-$ atoms

Valeriy Yazkov[1,*] on behalf of the DIRAC collaboration

[1]D. V. Skobeltsyn Institute of Nuclear Physics, M. V. Lomonosov Moscow State University, Leninskie Gory 1, 119991 Moscow, Russia

Abstract. Experiment DIRAC at CERN PS detects 349 ± 62 pairs from $\pi^- K^+$ and $\pi^+ K^-$ atoms and makes observation of exotic atoms consist of pion and kaon. It allows to measure a difference of S-wave pion-kaon scattering length with isospin 1/2 and 3/2: $|a_0^{1/2} - a_0^{3/2}|$. Values of pion-kaon scattering lengths are predicted in a frame of ChPT and LQCD. Therefore investigation of $\pi^- K^+$ and $\pi^+ K^-$ atoms gives possibility to check these predictions for simplest hadron-hadron system with *s*-quark.

1 Introduction

πK-atom ($A_{\pi K}$) is a hydrogen-like atom consisting of K^+ (K^-) and π^- (π^+) mesons with a Bohr radius of $a_B = 249$ fm, Bohr momentum of $p_B \simeq 0.8$ MeV/c and a ground state Coulomb binding energy of $E_B = 2.9$ keV .

The πK-atom lifetime (in ground state 1S), $\tau = \frac{1}{\Gamma}$ is dominated by the annihilation process into $\pi^0 K^0$ ($\pi^0 \bar{K}^0$). There is a relation between the width of $A_{\pi K}$ decay and S-wave πK scattering lengths for isospin 1/2 ($a_0^{1/2}$) and 3/2 ($a_0^{3/2}$) [1]:

$$\Gamma_{1S,\pi^0 K^0} = \frac{1}{\tau_{1S}} = 8\alpha^3 \mu^2 p^* (a_0^-)^2 (1 + \delta_K). \tag{1}$$

Here S-wave isospin-odd πK scattering length $a_0^- = \frac{1}{3}(a_0^{1/2} - a_0^{3/2})$ is defined in pure QCD for the quark masses $m_u = m_d$, α is the fine structure constant, μ is the reduced mass of the $\pi^\pm K^\mp$ system, p^* is the outgoing π^0 momentum in the πK atom system, and δ_K accounts for corrections, due to isospin breaking, at order α and quark mass difference ($m_u - m_d$).

Chiral Perturbation Theory (ChPT) describes QCD processes at low energies. ChPT in 1-loop approximation predicts S-wave pion-kaon scattering lengths [2, 3]:

$$a_0^{1/2} = 0.19 \pm 0.2,\ a_0^{3/2} = -0.05 \pm 0.02,\ a_0^{1/2} - a_0^{3/2} = 0.23 \pm 0.01 \tag{2}$$

in units of inverse pion mass.

ChPT with $L^{(2)}, L^{(4)}, L^{(6)}$ in 2-loop approximation predicts S-wave scattering length difference [4]:

$$a_0^{1/2} - a_0^{3/2} = 0.267\,. \tag{3}$$

Scattering length difference also has been predicted with dispersion analysis, using Roy-Steiner equations and experimental data in GeV range [5]:

$$a_0^{1/2} - a_0^{3/2} = 0.269 \pm 0.015\,. \tag{4}$$

*e-mail: valeri.yazkov@cern.ch

In the framework of lattice QCD, predictions for πK scattering length and their combination a_0^- have been obtained: $a_0^{1/2} = 0.1725^{+0.0026}_{-0.0157}$, $a_0^{3/2} = -0.0574^{+0.0029}_{-0.0060}$ [6], $a_0^{1/2} = 0.183 \pm 0.039$, $a_0^{3/2} = -0.0602 \pm 0.0040$ [7], $a_0^- = \frac{1}{3}(a_0^{1/2} - a_0^{3/2}) = 0.0811 \pm 0.0143$ [8], $a_0^- = \frac{1}{3}(a_0^{1/2} - a_0^{3/2}) = 0.0745 \pm 0.0020$ [9].

Prediction of scattering length difference in (4) together with $\delta_K = 0.040 \pm 0.022$ [1] provides (1) an estimation of lifetime of $A_{\pi K}$ in ground state:

$$\tau = (3.5 \pm 0.4) \times 10^{-15} \,. \tag{5}$$

There is differences in predictions of $a_0^{1/2} - a_0^{3/2}$ value, obtained with ChPT and Roy-Steiner equation [4, 5] from one side and LQCD [6, 9] from another side. It is needed to test predictions experimentally and accuracy of experimental measurement is to be at the level 5%.

The measurement of the S-wave πK scattering lengths would test our understanding of the chiral $SU(3)_L \times SU(3)_R$ symmetry breaking of QCD (u, d and s quarks), while the measurement of $\pi\pi$ scattering lengths checks only the $SU(2)_L \times SU(2)_R$ symmetry breaking (u, d quarks). This is the principal difference between $\pi\pi$ and πK scattering.

Experimental data on the πK low-energy phases are absent. The only experimental pion-kaon scattering length measurement has been done with estimation of πK atom lifetime, using data collected in 2008-2010 with Nickel (Ni) target [10]:

$$|a_0^-| M_\pi = 0.107^{+0.093}_{-0.035} \,. \tag{6}$$

Using all the data since 2007 and optimizing data handling and analysis, the observation of the πK atom could be achieved for the first time with a significance of more than 5 standard deviations [11]. On the basis of the same data sample, πK atom lifetime and πK S-wave isospin-odd scattering length have been measured with improved accuracy [12].

2 Method of πK atom observation and investigation

A method of investigation for $\pi^+\pi^-$, πK and other atoms, consisted of two oppositely charged mesons, has been proposed in [13]. Pairs of K^+ (K^-) and π^- (π^+) mesons are producing in proton-target interactions. Pairs, which are generated from fragmentation and strong decays ("short-lived" sources), are affected by Coulomb interaction in the final state. Some of them form Coulomb bound states — atoms, other are generated as free pairs ("Coulomb pairs"). Number of produced atoms (N_A) is proportional to a number of "Coulomb pairs" (N_C) with low relative momentum Q in a pair C.M. system: $N_A = K \cdot N_C$. The coefficient K is calculated with an accuracy better than 1% [14].

If at least one meson is generated from long-lived sources (electromagnetically or weakly decaying mesons or baryons: $\eta, \eta', K_s^0, \ldots$), then such pairs ("non-Coulomb pairs") are not affected by interaction in the final states.

After production, $A_{\pi K}$ travel through the target and could to annihilate into $\pi^0 K^0$, or to be ionised due to interaction with the target matter, producing specific "atomic pairs". These pairs have small relative momentum ($Q < 3$ MeV/c) and a number of such pairs n_A could be measured experimentally. Ratio of "atomic pair" number to a number of produced atoms is a breakup probability: $P_{\rm br}(\tau) = n_A/N_A = n_A/(K \cdot N_C)$ [15, 16]. In Fig 1 dependence of $A_{\pi K}$ breakup probability is shown for two Ni target are used in experiment DIRAC for pair laboratory momentum range $5.1 \div 8.5$ GeV/c. Value is averaged, using experimentally measured spectrum of atoms.

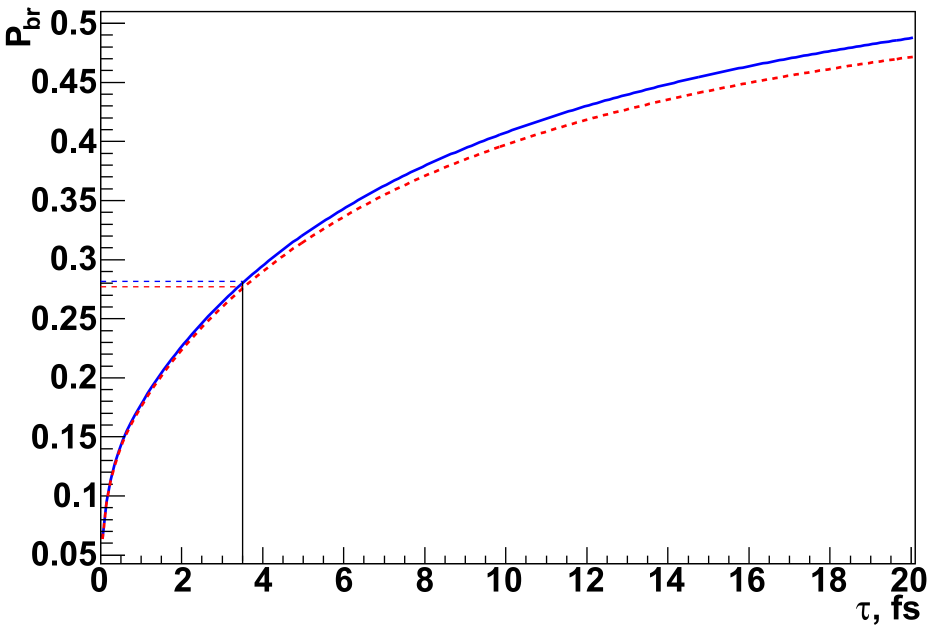

Figure 1. Dependence of the breakup probability $P_{\rm br}$ on $A_{\pi K}$ lifetime for 108μm (solid blue line) and 98μm (dashed red line) Ni targets, and an example how lifetime could be obtained from experimentally measured breakup probability

3 DIRAC setup

DIRAC setup was created to detect $\pi^+\pi^-$ with small relative momenta [17]. In 2004-2006 it has been modified in order to detect both $\pi^+\pi^-$ and πK pairs [18]. New detectors for particle identification have been added: Cherenkov detectors with heavy gas and aerogel for identification of K-mesons among background of pions and protons, correspondingly. Taking into account kinematic of πK "atomic pairs", new detectors cover only internal parts of each arm (see Fig. 2). Aerogel Cherenkov detector is mounted only in positive particle arm, because a flux of antiprotons is small relative to a flux of K^- mesons.

4 Selection πK events

Analysis procedure selects events which have signals of detectors expected for π^+K^- and π^-K^+ pairs. Fig. 3a presents the distribution of selected events over the difference of the particle production times for K^+ mesons in the range (4.4–4.5) GeV/c. The distribution is fitted by the simulated distribution of π^-K^+, $\pi^+\pi^-$, pπ^- and accidental pairs. Fig. 3b shows the fit for K^+ in the range (5.4–5.5) GeV/c. The contribution of misidentified pairs was estimated and accordingly subtracted [19]. Fraction of non-suppressed background pairs is calculated as function of momentum and used for estimation of systematic uncertainty (see below).

Fig. 4a illustrates the Q_L distribution of potential π^-K^+ pairs requiring a ChF signal and $Q_T < 4$ MeV/c. The dominant peak on the left side is due to pπ^- pairs from Λ decay. After requesting a ChA signal, the admixture of pπ^- pairs is decreased by a factor of 10 (Fig. 4b). By selecting proper TOFs between target and VH, background pπ^- and $\pi^+\pi^-$ pairs

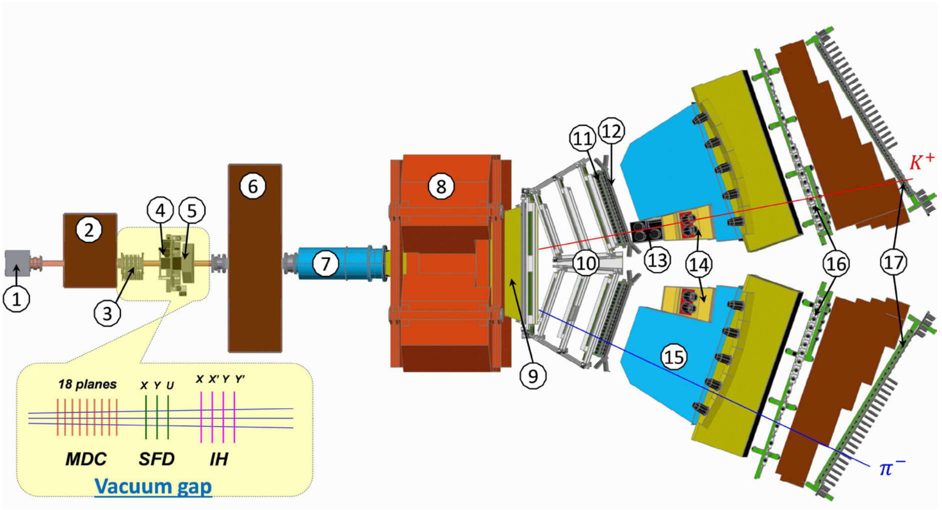

Figure 2. General view of upgraded DIRAC setup (1 – target station; 2 – first shielding; 3 – micro drift chambers (MDC); 4 – scintillating fiber detector (SFD); 5 – ionization hodoscope (IH); 6 – second shielding; 7 – vacuum tube; 8 – spectrometer magnet; 9 – vacuum chamber; 10 – drift chambers (DC); 11 – vertical hodoscope (VH); 12 – horizontal hodoscope (HH); 13 – aerogel Cherenkov detector (ChA); 14 – heavy gas Cherenkov detector (ChF); 15 – nitrogen Cherenkov detector (ChN); 16 – preshower detector (PSh); 17 – muon detector (Mu).

is substantially suppressed (Fig. 4c). In the final distribution, the well-defined $\pi^- K^+$ Coulomb peak at $Q_L = 0$ emerges beside the strongly reduced peak from Λ decays at $Q_L = -30$ MeV/c. The Q_L distribution of potential $\pi^+ K^-$ pairs shows a similar behavior. Applying the ChF and TOF criteria provides a sufficient background rejection. Fig. 5 presents the $\pi^+ K^-$ Coulomb peak at $Q_L = 0$ and a second peak from $\bar{\Lambda}$ decays at $Q_L = 30$ MeV/c.

For the final analysis, the DIRAC procedure selects events fulfilling the following criteria:

$$Q_T < 4\text{MeV}/c, |Q_L| < 20\text{MeV}/c\,.$$

5 Observation of $\pi^+ K^-$ and $\pi^- K^+$ atoms

Distributions of experimental data over relative momentum Q and its projections Q_L and Q_T have been fitted by a sum of simulated distributions of “atomic”, “Coulomb” and “non-Coulomb” pairs [12]. Contributions of simulated distributions are free parameters of fit. In order to reproduce distribution of experimental pairs over relative momentum Q and its projections, simulation procedure takes into account resolution and efficiency of the setup detectors, multiplicity of background particles and noise signals, multiple scattering in Pt (run 2007) and Ni (2008-2010) targets, detector planes and partitions.

Fig. 6a presents the experimental and simulated Q distributions of $\pi^- K^+$ and $\pi^+ K^-$ pairs for the data obtained from the Pt target and Ni targets. One observes an excess of events above the sum of “Coulomb” and “non-Coulomb” pairs in the low Q region, where atomic pairs are expected: these excess spectrum is shown in Fig. 6b together with the simulated distribution of atomic pairs. Comparing the experimental with the simulated distributions, demonstrates good agreement.

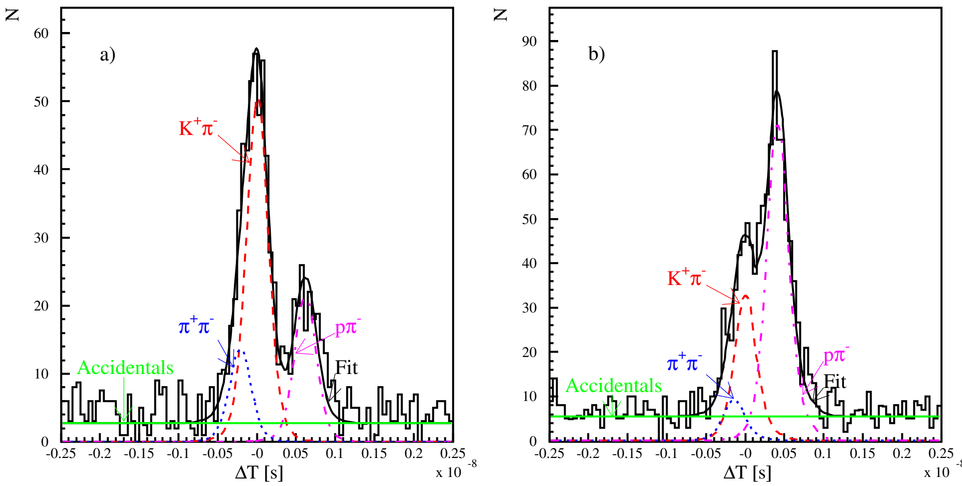

Figure 3. a) difference of particle generation times for events with positively charged particle momenta $(4.4 \div 4.5)$ GeV$/c$. Experimental data (histogram) are fitted by the event sum (black, solid): $\pi^- K^+$ (red, dashed), $\pi^+\pi^-$ (blue, dotted), pπ^- (magenta, dotted-dashed) and accidentals (green, constant). b) similar distributions for events with positively charged particle momenta $(5.4 \div 5.5)$ GeV$/c$.

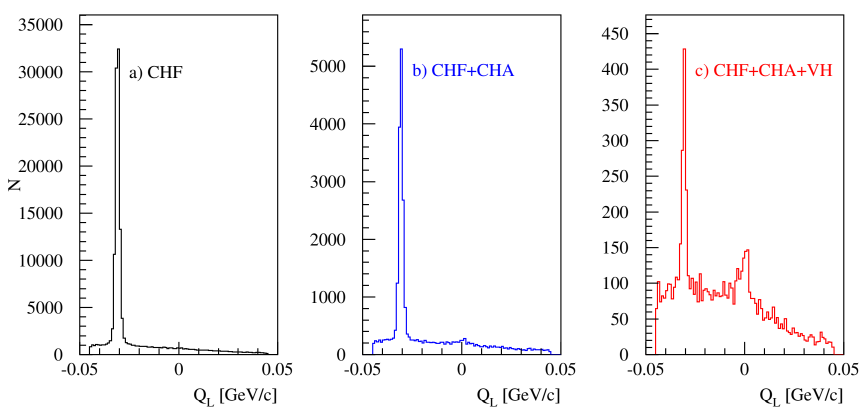

Figure 4. Q_L distribution of $\pi^- K^+$ pairs after applying different criteria: absence of signals in CHF and CHA detectors, proper TOFs between target and VH.

The numbers of atomic pairs, found in the $\pi^- K^+$ and $\pi^+ K^-$ data, are $n_A(\pi^- K^+) = 243 \pm 51$ ($\chi^2/n = 36/37$, n = number of degrees of freedom) and $n_A(\pi^+ K^-) = 106 \pm 32$ ($\chi^2/n = 42/37$). Total number of "atomic pairs" is $n_A(\pi K) = 349 \pm 61$ ($\chi^2/n = 41/37$). Quality of $\pi^- K^+$ and $\pi^+ K^-$ data fit, performed in assumption that "atomic pairs" are absent, is worse: $\chi^2/n = 73/38$.

Numbers of $\pi^+ K^-$ and $\pi^- K^+$ "atomic pairs" obtained with analysis of one-dimensional distributions over Q and $|Q_L|$ and two-dimensional $(|Q_L|, Q_T)$ distribution are presented in

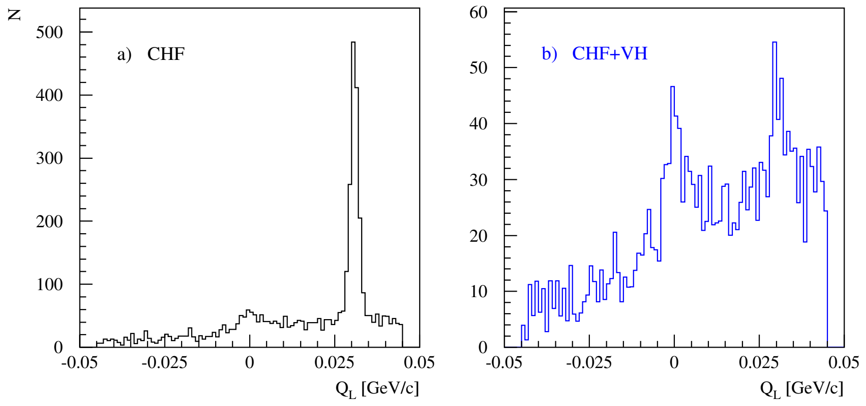

Figure 5. Q_L distribution of π^+K^- pairs after applying different criteria: absence of signals in CHF detector, proper TOFs between target and VH.

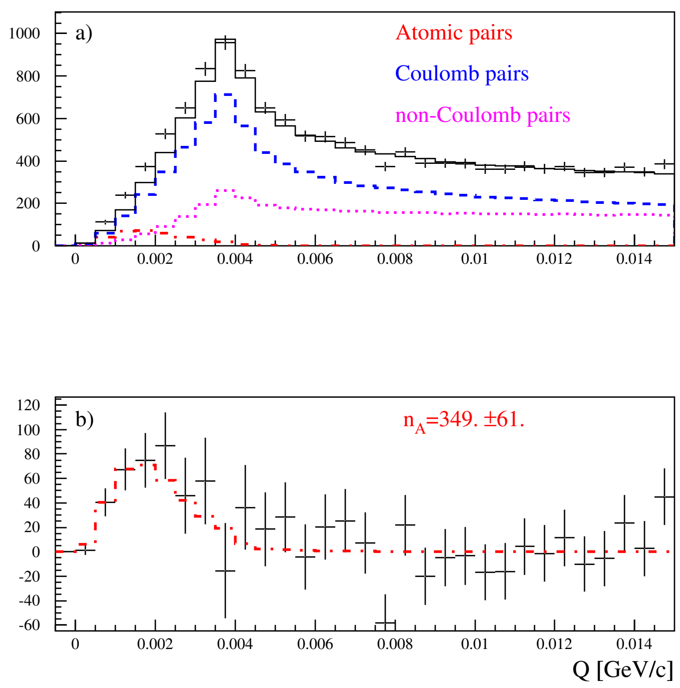

Figure 6. a) Distribution of π^+K^- and π^-K^+ pairs over Q, shown by points with error bars, is fitted by a sum of simulated distributions of “atomic” (red dotted-dashed), “Coulomb” (blue dashed) and “non-Coulomb” (magenta dotted) distributions. A sum of background distributions (“Coulomb” and “non-Coulomb”) is shown by a solid black line. b) Difference of experimental and background distributions is shown together with simulated distributions of “atomic pairs”.

Table 1 (Ni and Pt target together). The best statistical accuracy is achieved by analysis of Q and $(|Q_L|, Q_T)$ distributions. Signal to error ratio is more than 5. The 1-dimensional $|Q_L|$ analysis for all πK data yields $n_A = 230\pm92$, which does not contradict the values, obtained in the other two statistically more precise analyses. Compared to the previous investigation [20], the Pt data was analysed including the upstream detectors. The consequence is a decrease of the statistics, but on the other hand an increase of the Q_T resolution. This better resolution

Table 1. "Atomic pair" numbers n_A obtained by analyzing the 1-dimensional Q and $|Q_L|$ distributions and the 2-dimensional ($|Q_L|$, Q_T) distribution. Only statistical errors are given.

Analysis	$\pi^- K^+$	$\pi^+ K^-$	$\pi^- K^+$ and $\pi^+ K^-$
Q	243 ± 51 (4.7σ)	106 ± 32 (3.3σ)	349 ± 61 (5.7σ)
$\lvert Q_L \rvert$	164 ± 79 (2.1σ)	67 ± 47 (1.4σ)	230 ± 92 (2.5σ)
$\lvert Q_L \rvert$, Q_T	237 ± 50 (4.7σ)	78 ± 32 (2.5σ)	314 ± 59 (5.3σ)

Table 2. Estimations of systematic errors, which are induced by different sources, for analysis of data distribution over relative momentum Q, its longitudinal projection $|Q_L|$ and two dimensional distribution over ($|Q_L|$, Q_T).

Sources of systematic errors	σ_Q^{syst}	$\sigma_{Q_L}^{syst}$	$\sigma_{\lvert Q_L \rvert, Q_T}^{syst}$
Uncertainty in Λ width correction	0.8	3.0	2.0
Uncertainty of multiple scattering in Ni (Pt) target	4.4	0.7	2.7
Accuracy of SFD simulation	0.2	0.0	0.1
Correction of Coulomb correlation function due to finite size production region	0.0	0.2	0.1
Uncertainty in πK pair laboratory momentum spectrum	3.3	5.4	7.8
Uncertainty in laboratory momentum spectrum of background pairs	6.6	1.6	5.4
Total	8.6	6.4	10.1

improves the quality of data. Concerning the Ni target, the increase of n_A, compared to [10], is caused by optimizing the time-of-flight criteria, which decreases "atomic pair" losses for the same fraction of background in the final distributions.

The evaluation of the "atomic pair" number n_A is affected by several sources of systematic errors [19, 21]. These uncertainties lead to differences in the shapes of experimental and MC distributions for "atomic", "Coulomb" and to a much lesser extent for "non-Coulomb" pairs. The shape differences induce a bias in the value of the fit parameter n_A, corresponding to a systematic error of the "atomic pair" number. Sources of systematic error and estimation of error values are listed in Table 2.

Taking into account both statistical and systematic errors, the one-dimensional $\pi^\pm K^\mp$ analysis in Q yields $n_A = 349 \pm 61(stat) \pm 9(syst) = 349 \pm 62(tot)$ "atomic pairs" (5.6 σ) for both combinations of charge and two-dimensional analysis in ($|Q_L|$, Q_T) yields $n_A = 314 \pm 59(stat) \pm 10(syst) = 314 \pm 60(tot)$ "atomic pairs" (5.2 σ). This is the first statistically significant observation πK atom — the dimesonic Coulomb bound states involving strangeness.

6 Measurement of S-wave isospin-odd πK scattering length

Experimentally measured numbers of "atomic pairs" n_A and produced atoms N_A allow (see section 2) to obtain breakup probability $P_{\rm br}$.

Table 3 contains the $P_{\rm br}$ values obtained in the Q and ($|Q_L|$,Q_T) analyses with statistical uncertainties.

Table 3. Experimental $P_{\rm br}$ from Q and $(|Q_L|, Q_T)$ analyses. Only statistical uncertainties are cited.

Data	RUN	Target (μm)	P_{br}^{Q}	$P_{br}^{\|Q_L\|,Q_T}$
π^+K^-	2007	Pt (25.7)	1.2 ± 1.3	0.27 ± 0.56
π^+K^-	2008	Ni (98)	0.53 ± 0.39	0.42 ± 0.38
π^+K^-	2009	Ni (108)	0.29 ± 0.20	0.33 ± 0.24
π^+K^-	2010	Ni (108)	0.33 ± 0.22	0.21 ± 0.20
π^-K^+	2007	Pt (25.7)	1.09 ± 0.52	1.44 ± 0.59
π^-K^+	2008	Ni (98)	0.32 ± 0.20	0.44 ± 0.22
π^-K^+	2009	Ni (108)	0.23 ± 0.16	0.16 ± 0.15
π^-K^+	2010	Ni (108)	0.41 ± 0.17	0.34 ± 0.16
$\pi^+K^-\&\pi^-K^+$	2007	Pt, 25.7	1.11 ± 0.48	0.83 ± 0.41

Sources of systematic uncertainties of breakup probability are mainly the same like for number of “atomic pairs” (see Table 2). There only one new source - uncertainty in the $P_{\rm br}(\tau)$ relation.

Estimations of systematic errors, induced by different sources [12], are presented in Table 4. The total errors were calculated as the quadratic sum. The procedure of the πK atom lifetime estimation, described below, includes all systematic errors, although their contributions are insignificant compared to the statistical errors.

Table 4. Estimated systematic errors of $P_{\rm br}$ for data collected with Pt and Ni targets in Q and $(|Q_L|, Q_T)$ analyses.

Source	Q		$(\|Q_L\|, Q_T)$	
	Pt	Ni	Pt	Ni
Uncertainty in Λ width correction	0.011	0.0006	0.073	0.0006
Uncertainty of multiple scattering in the target	0.0087	0.0051	0.014	0.0036
Accuracy of SFD simulation	0.	0.0002	0.	0.0003
Correction of the Coulomb correlation function on finite size production region	0.0001	0.0001	0.0002	0.0000
Uncertainty in πK pair lab. momentum spectrum	0.089	0.0052	0.25	0.0050
Uncertainty in the laboratory momentum spectrum of background pairs	0.22	0.0011	0.21	0.0011
Uncertainty in the $P_{\rm br}(\tau)$ relation	0.01	0.0055	0.01	0.0055
Total	0.24	0.0092	0.34	0.0084

For estimating the lifetime of $A_{\pi K}$ in the ground state, the maximum likelihood method [22] is applied [23]:

$$L(\tau) = \exp\left(-U^T G^{-1} U/2\right), \tag{7}$$

where $U_i = \Pi_i - P_{{\rm br},i}(\tau)$ is a vector of differences between measured Π_i ($P_{\rm br}$ in Table 3) and corresponding theoretical breakup probability $P_{{\rm br},i}(\tau)$ for a data sample i. The error matrix of U, named G, includes statistical (σ_i) as well as systematic uncertainties. Only the term corresponding to the uncertainty in the $P_{\rm br}(\tau)$ relation is considered as correlated between the Ni and Pt data, which is a conservative approach and overestimates this error. The other systematic uncertainties do not exhibit a correlation between the data samples from the Ni and Pt targets. On the other hand, systematic uncertainties of the Ni data samples are correlated. The likelihood functions of the $(|Q_L|, Q_T)$ and Q analyses are shown in Fig. 7.

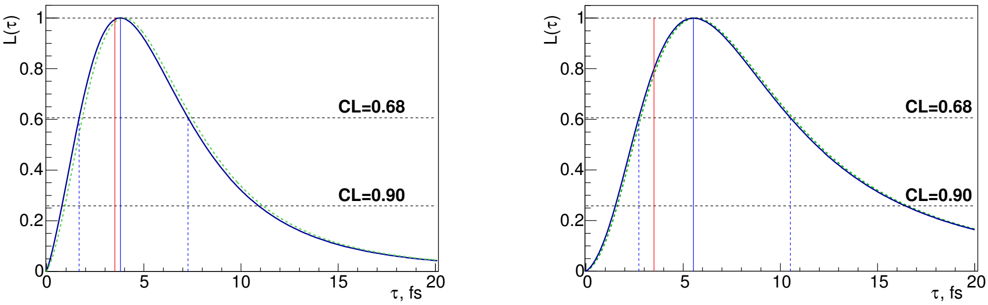

Figure 7. Likelihood functions $L(\tau)$ for $(|Q_L|, Q_T)$ (left) and Q (right) analyses with $Q_T < 4$ MeV/c. The likelihood functions on the basis of both statistical and systematic errors (dashed green line) and on the basis of only statistical error (solid blue line) are presented. The vertical blue lines indicate the best estimate for $\tau_{\rm tot}$ and the corresponding confidence interval. The vertical red line is the theoretical prediction (5).

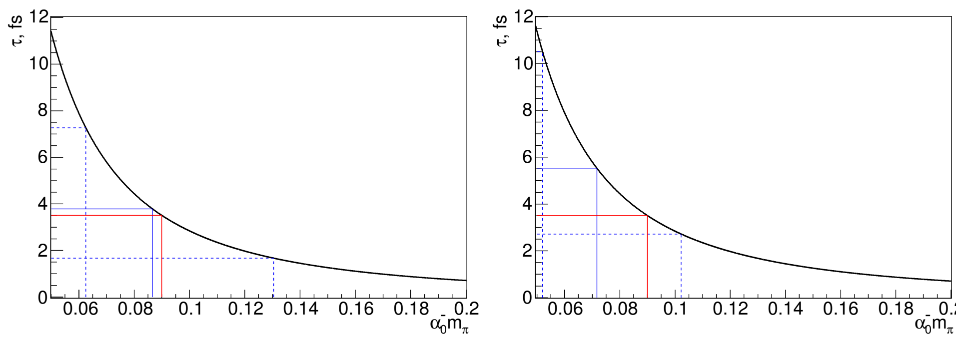

Figure 8. Ground state $A_{\pi K}$ lifetime τ_{1S} versus a_0^-. Experimental results (blue lines) are compared to the theoretical prediction (red lines). $(|Q_L|, Q_T)$ analysis (left) and Q analysis (right).

New estimation of $A_{\pi K}$ lifetime in ground state, based on two-dimensional analysis in $(|Q_L|, Q_T)$ [12]:

$$\tau = (3.8^{+3.3}_{-2.0}|_{stat}\ ^{+1.0}_{-0.6}|_{syst})\ \text{fs} = (3.8^{+3.5}_{-2.1}|_{tot})\ \text{fs}\,, \tag{8}$$

which corresponds (see Fig. 8(left)) to isospin-odd πK scattering length estimation to be:

$$|a_0^-|M_\pi = 0.087^{+0.043}_{-0.024}|_{tot}\,. \tag{9}$$

Estimation, based on Q analysis [12]:

$$\tau = (5.5^{+4.9}_{-2.8}|_{stat}\ ^{+0.9}_{-0.5}|_{syst})\ \text{fs} = (5.5^{+5.0}_{-2.8}|_{tot})\ \text{fs}\,, \tag{10}$$

provides (see Fig. 8(right)) the following value of the πK scattering length a_0^-:

$$|a_0^-|M_\pi = 0.072^{+0.031}_{-0.020}|_{tot}\,. \tag{11}$$

Measured values are compatible with theoretical predictions, taking into account the experimental precision.

7 Summary

In the DIRAC experiment at CERN, the dimesonic Coulomb bound states involving strangeness, the $\pi^- K^+$ and $\pi^+ K^-$ atoms, were observed for the first time with reliable statistics. The one-dimensional $\pi^\pm K^\mp$ analysis in Q yields 349 ± 62(*tot*) "atomic pairs" (5.6 σ) for both combinations of charge. Analogously, a two-dimensional analysis in $(|Q_L|, Q_T)$ was performed with the result of 314 ± 60(*tot*) "atomic pairs" (5.2 σ).

The breakup probabilities for each atom type and each target are determined. By means of these probabilities, the lifetime of the πK atom in the ground state is evaluated to be:

$$\tau_{\rm tot} = (5.5^{+5.0}_{-2.8}\big|_{\rm tot}) \cdot 10^{-15}\,{\rm s}\,,$$

and the S-wave isospin-odd πK scattering length deduced:

$$\left|a_0^-\right| = \frac{1}{3}\left|a_0^{1/2} - a_0^{3/2}\right| = (0.072^{+0.031}_{-0.020}\big|_{\rm tot}) M_\pi^{-1}\,.$$

We are grateful to CERN for support and the PS team for the excellent performance of the accelerator. This work was funded by CERN, INFN (Italy), INCITE and MICINN (Spain), IFIN-HH (Romania), the Ministry of Education and Science and RFBR grant 01-02-17756-a (Russia), the Grant-in-Aid from JSPS and Sentanken-grant from Kyoto Sangyo University (Japan).

References

[1] J. Schweizer, Phys. Lett. B **587**, 33 (2004)
[2] V. Bernard *et al.*, Phys. Rev. D **43**, 2757 (1991)
[3] A. Roessl, Nucl. Phys. B **555**, 507 (1999)
[4] J. Bijnens *et al.*, JHEP **0405**, 036 (2004)
[5] P. Buttiker *et al.*, Eur. Phys. J. C **33**, 409 (2004)
[6] S.R. Beane *et al.*, Phys. Rev. D **77**, 094507 (2008)
[7] C.B. Lang *et al.*, Phys. Rev. D **86**, 054508 (2012)
[8] K. Sasaki *et al.*, Phys. Rev. D **89**, 054502 (2014)
[9] T. Janowski et al., PoS *LATTICE2014* 080 (2015)
[10] B. Adeva *et al.*, Phys. Lett. B **735**, 288 (2014)
[11] B. Adeva *et al.*, Phys. Rev. Lett. **117**, 112001 (2016)
[12] B. Adeva *et al.*, Phys. Rev. D **96**, 052002 (2017)
[13] L. Nemenov, Sov. J. Nucl. Phys. **41**, 629 (1985)
[14] L. Afanasyev and O. Voskresenskaya, Phys. Lett. B **453**, 302 (1999)
[15] L. Afanasyev and A. Tarasov, Phys. At. Nucl. **59**, 2130 (1996)
[16] M. Zhabitsky, Phys. At. Nucl. **71**, 1040 (2008)
[17] B. Adeva *et al.*, Nucl. Instrum. Methods A **515**, 467 (2003)
[18] B. Adeva *et al.*, Nucl. Instrum. Methods A **839**, 52 (2016)
[19] V. Yazkov and M. Zhabitsky, DN **2013-06** (DN = DIRAC Note), cds.cern.ch/record/1628544
[20] B. Adeva *et al.*, Phys. Lett. B **674**, 11 (2009)
[21] A. Benelli and V. Yazkov, DN **2016-01**, cds.cern.ch/record/2137645
[22] D. Drijard and M. Zhabitsky, DN **2008-07**, cds.cern.ch/record/1367888
[23] V. Yazkov and M. Zhabitsky, DN **2016-06**, cds.cern.ch/record/2252375